Clarification of the Mechanism of Unintentional Radiated Emissions from Unshielded Twisted Pair Cable

Shun IGARASHI*, Daisuke MIYAWAKI, Suguru YAMAGISHI, Ichiro KUWAYAMA, Kengo IOKIBE, and Yoshitaka TOYOTA

Communication frequency in telecommunications has been increasing to improve data transmission speed and capacity. However, this increase also raises the possibility of unintentional radiated emissions from communication cables, leading to electromagnetic compatibility (EMC) problems. From the viewpoint of radiation, we examined the transmission and radiation characteristics of unshielded twisted pair (UTP) cable commonly used in local area networks and in-vehicle communication networks. The examination confirmed that the UTP cable emits a portion of the transmitting signal within a certain frequency band. This emission follows the same mechanism as a leaky cable. We verified that the equation derived from the leaky cable mechanism can explain the relationship between the radiation bandwidth and the radiation angle. This paper introduces the radiated emission from UTP cable and explains the radiation mechanism in detail. Additionally, we provide a guideline on how to avoid potential EMC problem related to UTP cable.

Keywords: unshielded twisted pair cable, UTP cable, EMC, unintentional electromagnetic radiation

1. Introduction

Recently, frequency bands used in wireless communication systems have been getting higher and wider, as exemplified by the full-scale launch of 5th Generation Mobile Communication System (5G) services.[1] There is the same trend in automobiles. In-vehicle and outside-vehicle communication frequencies have been getting higher to improve data rate and capacity with low latency for achieving fully automated driving.[2] Under these circumstances, cables may serve as the sources of generation and inflow of electromagnetic noise that may cause electromagnetic compatibility (EMC*1) problems, which did not arise in previous communication systems. Therefore, it is important to select cables that emit or receive minimal electromagnetic noise.

An unshielded twisted pair (UTP) cable, in which two electric wires are helically twisted, is considered to emit and receive minimal electromagnetic noise because currents flowing in the electric wires cancel the magnetic fields around the cable.[3] UTP cables are, therefore, widely used for wiring of conventional LAN systems and in-vehicle communication systems. On the other hand, we developed and applied twisted pair leaky cables, whose structure was similar to that of UTP cables, to communication antennas in tunnels.[4] In line with the recent trend to use higher frequencies for communication devices, we considered that UTP cables were likely to cause unexpected EMC problems.

With this backdrop, the authors evaluated the transmission characteristics of high-frequency signals in anticipation of using UTP cables for transmitting signals of multi-gigabit*2 or higher. Through the evaluation, we confirmed that unintentional electromagnetic radiation occurred in a certain frequency bands.[5],[6] We found that radiation from UTP cables occurred in the same mechanism as that of leaky cables due to their structural similarity with leaky cables and that the radiation band and radiation direction can be described using the equation for leaky cables. This paper presents the evaluation results of the transmission and radiation characteristics when high-frequency signals are input into a UTP cable and explains the radiation mechanism based on that of leaky cables. We also propose guidelines for selecting UTP cables that are less likely to cause EMC problems from the viewpoint of emitting and receiving noise.

2. Transmission Characteristics of a UTP Cable

UTP cables are used for wiring to transmit differential signals,*3 which are transmitted and received between devices. The basic electrical characteristics are evaluated based on the transmission characteristics and reflection characteristics against the input differential signals. To enable communication between devices, it is desirable to attain low loss and low reflection. The authors examined a UTP cable, which is generally used for in-vehicle communication wiring. The structure and dimensions of this UTP cable are as shown in Fig. 1.[5],[6] The structure is character-

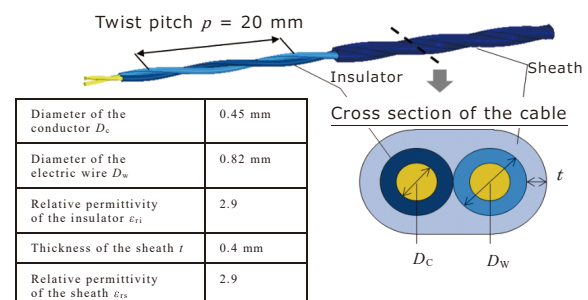| Diameter of the conductor D_c	0.45 mm
Diameter of the electric wire D_w	0.82 mm
Relative permittivity of the insulator ε_{ri}	2.9
Thickness of the sheath t	0.4 mm
Relative permittivity of the sheath ε_{rs}	2.9

Fig. 1. Structure and dimensions of a UTP cable

ized by two helically twisted electric wires. The twisted shape of an entire cable is maintained by the resin (sheath).

We evaluated the transmission characteristics and reflection characteristics of the UTP cable when high-frequency differential signals of up to 10 GHz were input using the measurement system indicated in Figs. 2 (a) and 2 (b). A UTP cable with a total length of 420 mm was wired at a height of 25 mm above ground. It was connected to a measuring instrument called a vector network analyzer*4 via a connection jig substrate.

(a) Measurement configuration

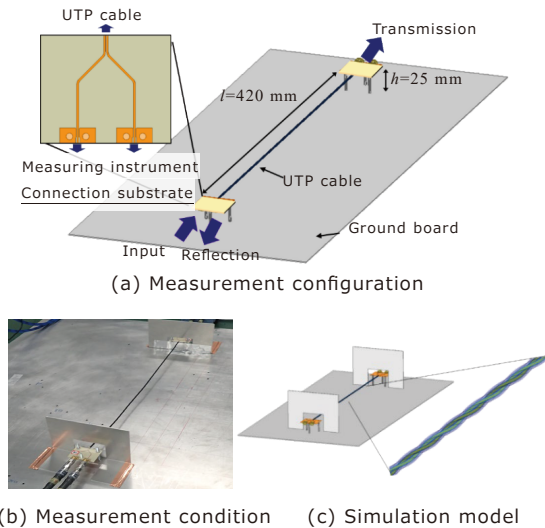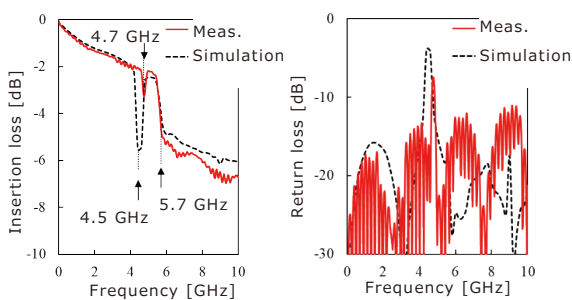(b) Measurement condition   (c) Simulation model

Fig. 2. Transmission and reflection characteristics evaluation system

Figure 3 shows the evaluation results of the transmission characteristics and reflection characteristics. The vertical axis indicates the ratio of the transmitted and reflected power against the input power in a logarithm. In terms of the transmission characteristics shown in Fig. 3 (a), the smaller the value, the higher the insertion loss. In terms of the reflection characteristics shown in Fig. 3 (b), the higher the value, the higher the return loss. The transmission characteristics of the UTP cable subject to measurement (indicated by the solid line in Fig. 3 (a)) indicate the general properties of a gradual increase in loss in line with a frequency increase up to 4 GHz. However, a peculiar increase in loss was observed in the frequency bands of

(a) Transmission characteristics   (b) Reflection characteristics

Fig. 3. Evaluation results of the transmission and reflection characteristics

around 4.7 GHz and 5.7 GHz or higher.

For the discussion based on electromagnetic field analysis in Chapter 3 and beyond, we conducted verification and confirmed that the electromagnetic field simulation reproduced this peculiar increase in loss. The measurement system was modeled using a three-dimensional electromagnetic field simulator (HFSS, ANSYS Inc.) (Fig. 2 (c)) to analyze the electrical characteristics of the UTP cable. The results are shown by the dashed line in Fig. 3. As in the case of the measurement results, the simulation results showed that the loss increased in the frequency band around 4.5 GHz and 5.7 GHz or higher.

First, we focus on the increase in loss around 4.5 GHz. Return loss increased sharply at 4.5 GHz (Fig. 3 (b)), resulting in an increase in insertion loss. In other words, of the power input into the UTP cable, the power that returned to the input end due to reflection increased, resulting in a decrease in the power that reached the output end (an increase in insertion loss). Given that the propagation wavelength at 4.5 GHz (40 mm) is equivalent to double the twist pitch (20 mm), the increase in return loss is attributable to reflection from each twisted wire mutually strengthened due to the in-phase synthesis (Fig. 4).
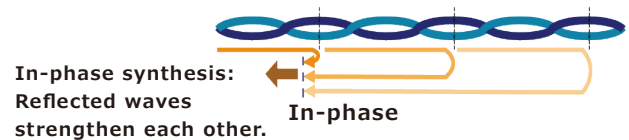

Fig. 4. Reflected waves mutually strengthened due to in-phase reflection

Meanwhile, at the frequency band of 5.7 GHz or higher, an increase in return loss equivalent to an increase in insertion loss did not occur. That is, although the power that returned to the input end due to reflection did not increase, the power that reached the output end decreased sharply. This is presumed to be caused by radiation of part of the power input into the UTP cable as electromagnetic waves during transmission.

3. Electromagnetic Radiation from the UTP Cable

3-1 Experimental verification

To verify that the increase in insertion loss described in the previous chapter was attributed to the radiation of electromagnetic waves, we measured the received power of an antenna placed next to the cable as shown in Fig. 5.[5],[6] To clarify that the radiation was attributed to the structure of the UTP cable, similar measurement was conducted on a two-parallel-wire cable for comparison.

Figure 6 shows the measurement results of the power received of the antenna. The higher the value, the higher the received power of the antenna, indicating that electromagnetic waves are emitted from the cable. The measurement results of the UTP cable (as shown by the solid line in Fig. 6) indicated a significant increase in the received

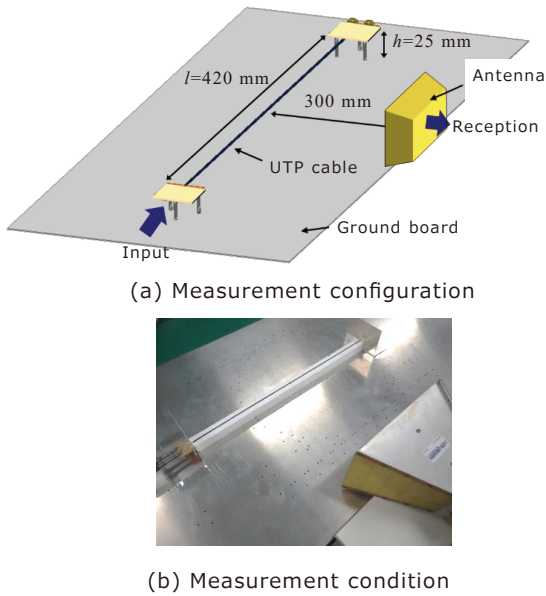(a) Measurement configuration

(b) Measurement condition

Fig. 5. Evaluation system for radiation from a cable

power of the antenna in the frequency band of 5.7 GHz or higher. It was directly confirmed that electromagnetic waves were emitted from the UTP cable in this frequency band, which corresponded to the frequency band in which insertion loss increased sharply as described in Section 2 (as indicated in Fig. 7 again). From the result, the increase
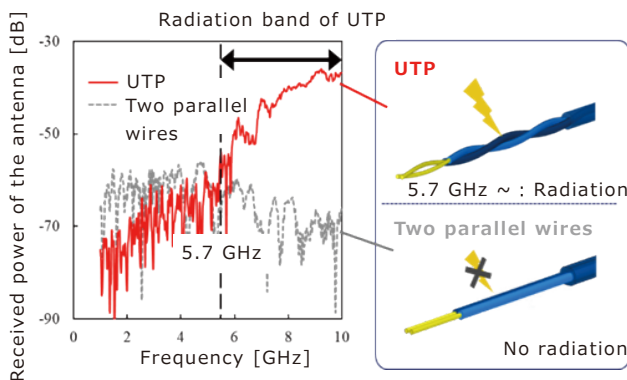

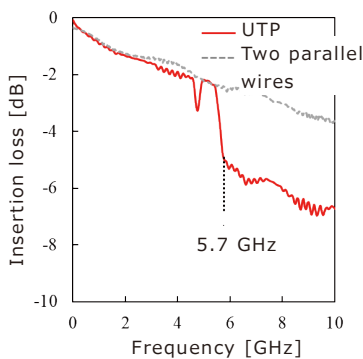Fig. 6. Measurement results of received power of the antenna

Fig. 7. Transmission characteristics of the UTP cable and the two-parallel-wire cable

in insertion loss can be attributed to the emission of electromagnetic waves.

On the other hand, the measurement results of the two-parallel-wire cable (indicated by the dashed line in Fig. 6) did not show a significant increase in the received power of the antenna nor a peculiar increase in transmission characteristics (as indicated by the dashed line in Fig. 7) measured in the configuration similar to that of Fig. 2. Thus, it was clear that no electromagnetic waves were emitted from the two-parallel-wire cable. Based on these results, we concluded that the electromagnetic radiation, which was observed in the band of 5.7 GHz or higher of the UTP cable, was attributed to the structure of the UTP cable.

3-2 Mechanism of radiation

Based on the structural similarity with leaky cables, the mechanism of radiation from a UTP cable is explained by applying the same concept[4] as that of leaky cables.[6] Leaky coaxial cables, which have been widely used as wireless communication antennas in tunnels and underground shopping malls, have slots (holes) at a certain intervals on their external conductor. When signals are input into a leaky coaxial cable, an electric field is generated in a slot. The electric field serves as a wave source to emit electromagnetic waves (Fig. 8). On the other hand, when differential signals are input into a UTP cable, an electric field is formed between the electric wires and this is equivalent to periodically aligned wave source at twist pitch as in the case of a leaky coaxial cable (Fig. 9).
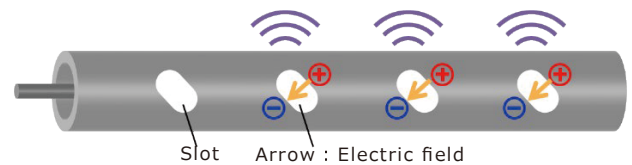

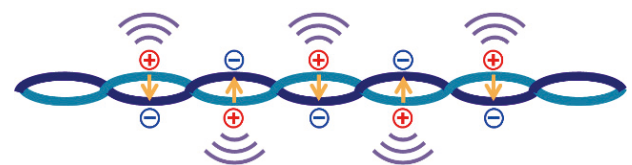Fig. 8. Working principle of radiation from a leaky coaxial cable

Fig. 9. Electric field formed in a UTP cable

In a structure where wave sources are arrayed at a certain period, electromagnetic waves are emitted in the direction which mutually strengthens electromagnetic waves from respective wave sources due to the in-phase synthesis. Here, we discuss the conditions under which electromagnetic waves emitted from wave sources arrayed at each twist pitch in a UTP cable become in-phase.

In Fig. 10, the electromagnetic waves emitted from point A and point B become in-phase at line AC when the electrical length[*5] of route AB + the electrical length of route BC matches the integer multiple of the wavelength. This can be expressed by Eq. (1) below.
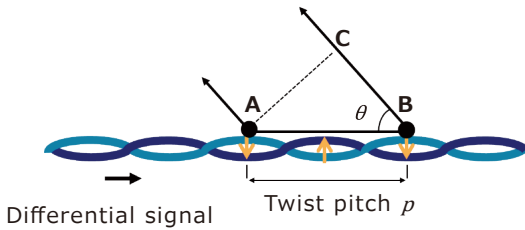
Clarification of the Mechanism of Unintentional Radiated Emissions from Unshielded Twisted Pair Cable

Fig. 10. In-phase conditions of electromagnetic waves from wave sources in a UTP cable

$$p\sqrt{\varepsilon_{\text{reff}}} + p\cos\theta = n\lambda_0 \quad \cdots\cdots\cdots\cdots\cdots\cdots (1)$$

Here, p is the twist pitch, $\varepsilon_{\text{reff}}$ is the effective relative permittivity[*6] for differential excitation, θ is the angle ABC (radiation angle), λ_0 is the free space wavelength, n is a natural number, the first term of the left side is the electrical length of route AB, and the second term is the electrical length of route BC.

Based on the relationship among the frequency f, speed of light c, and free space wavelength λ_0 ($f = c/\lambda_0$), Eq. (1) can be transformed as follows:

$$f = \frac{c}{p} \frac{n}{\sqrt{\varepsilon_{\text{reff}}} + \cos\theta} \quad \cdots\cdots\cdots\cdots\cdots\cdots\cdots (2)$$

Given that the possible value of the radiation angle is between 0° and 180°, the frequency band in which radiation occurs can be expressed in the following equation:

$$\frac{c}{p} \frac{n}{\sqrt{\varepsilon_{\text{reff}}} + 1} < f < \frac{c}{p} \frac{n}{\sqrt{\varepsilon_{\text{reff}}} - 1} \quad \cdots\cdots\cdots\cdots (3)$$

To compare with the radiation band measured in Section 3-1 (Fig. 6), the parameters of the UTP cable were applied to the Eq. (3) for calculation. The measurement results showed that the lower limit frequency at which radiation occurred was 5.7 GHz. Thus, calculation was focused on the lowest frequency band ($n = 1$). The twist pitch p is 20 mm, as shown in Fig. 1. For the effective relative permittivity, the value calculated in the cross-section analysis ($\varepsilon_{\text{reff}} = 2.7$) by the two-dimensional electromagnetic field analysis software (2D Extractor, ANSYS Inc.) was used. When these values were assigned to Eq. (3), the radiation band was 5.7 GHz $< f <$ 23 GHz. We confirmed that the lower limit frequency of the radiation band calculated by Eq. (3) matched the frequency at which radiation started to be observed in the experiment described in Section 3-1 (5.7 GHz).

The radiation angle can be expressed as follows by transforming Eq. (2):

$$\cos\theta = \frac{c}{p} \frac{1}{f} - \sqrt{\varepsilon_{\text{reff}}} \quad \cdots\cdots\cdots\cdots\cdots\cdots (4)$$

The equation shows that the radiation angle is dependent on the frequency, meaning that the higher the frequency, the greater the radiation angle θ. For example, based on the calculation results, the radiation angle of the UTP cable we evaluated in this paper was 31° at 6 GHz and 76° at 8 GHz.

3-3 Radiation electric field analysis based on simulation

To verify the frequency dependence of the radiation angle, we analyzed the electric field distribution when differential signals of different frequencies were input into the simulation model of Fig. 2.

Figure 11 (a) shows a top view of the simulation model, and Figs. 11 (b) to (d) show the simulation results of the electric field distribution on the x-y plane, including the UTP cable, at the respective frequencies. It should be noted that the differential signals were input from the left in the figure and that a common color scale was used for the electric field. At 3 GHz, which was outside the radiation band of Eq. (3), the electric field concentrated near the UTP cable, and no radiation was observed (Fig. 11 (b)). It was also confirmed that no radiation occurred at around 4.5 GHz, where insertion loss increased locally (not shown here).[5]

Meanwhile, as the frequency increased, radiation started to occur from 5.7 GHz, the lower limit frequency of the radiation band of Eq. (3) (refer to references (5) and (6) for the electric field distribution). At 6 GHz and 8 GHz within the radiation band, radiation occurred in obviously different directions (Figs. 11 (c) and (d)). The radiation angle calculated based on this electric field distribution is about 7° at 5.7 GHz (refer to references (5) and (6)), 31° at 6 GHz, and 76° at 8 GHz. They well matched the values calculated based on Eq. (4) in Section 3-2.

Based on the comparison between the equation and the actual measurement/simulation results discussed in Chapter 3, we confirmed that the radiation band and radiation angle from the UTP cable can be expressed by Eqs. (3) and (4), which are based on the radiation mechanism from leaky cables. We were able to explain the radiation from the UTP cable based on the same mechanism as that of leaky cables.
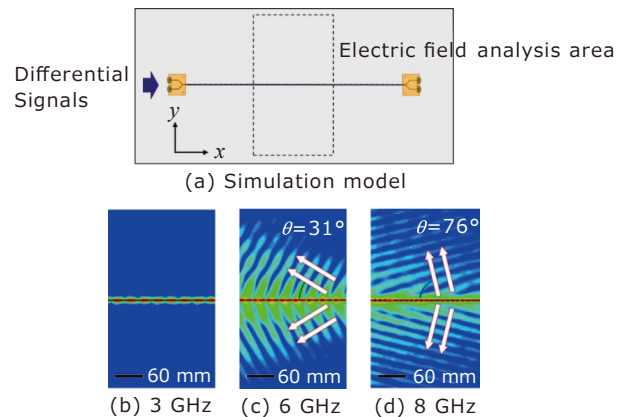

Fig. 11. Simulation results of the electric field distribution around the UTP cable

4. Measures against a Potential EMC Problem

Up to the previous chapter, we demonstrated that unintentional electromagnetic radiation occurs when differential signals of 5.7 GHz or higher are input into the UTP cable shown in Fig. 1. This means that the EMC problem caused by unintentional radiation can be avoided by restricting input signal frequency to less than 5.7 GHz. However, given the equivalence between the radiation characteristics and

receiving characteristics, this UTP cable is characterized by properties to easily receive electromagnetic noise of 5.7 GHz or higher, which is the radiation band.

In 5G, which has come into full-scale use for services and has been increasingly applied to in-vehicle communication devices, the sub-6 bands (3.7 GHz to 6.0 GHz) are used for wireless communication. UTP cables, which are used for wiring of in-vehicle communication, may be exposed to radio waves of the sub-6 bands. In other words, UTP cables are likely to receive radio waves of the sub-6 bands, which are emitted from 5G devices, as noise, and this is likely to hinder communication between devices connected by UTP cables. This potential EMC problem can be avoided by shifting the radiation band of UTP cables in use to frequencies higher than those of the sub-6 bands.

Based on Eq. (3), there are two possible methods to shift the radiation band: (i) reducing the effective relative permittivity for the differential excitation and (ii) reducing the twist pitch. Method (i) requires changes in the coating material and is difficult to use in actual applications. On the other hand, method (ii) can be achieved by changing the twisting conditions and is relatively feasible.

One possible measure is to change the twist pitch of the UTP cable shown in Fig. 1 from 20 mm to 15 mm. When the twist pitch is reduced to 15 mm, the radiation band calculated based on Eq. (3) is 7.6 GHz $< f <$ 31 GHz, which does not overlap the sub-6 bands.

We conducted an electromagnetic field analysis and confirmed that no radiation occurred at 6 GHz. Figure 12 shows the electric field distribution when differential signals of 6 GHz are input into UTP cables whose twist pitch is 20 mm and 15 mm. Radiation occurred at the twist pitch of 20 mm, as explained in Section 3-3 (Fig. 12 (a)). At the twist pitch of 15 mm, it was confirmed that the electric field concentrated around the cable (Fig. 12 (b)) as in the case where no radiation occurred in Section 3-3 (Fig. 11 (b)). Thus, the reduction of the twist pitch to 15 mm makes it possible to prevent the reception of electromagnetic noise of the sub-6 bands and avoid an EMC problem caused by an inflow of noise from the cable.

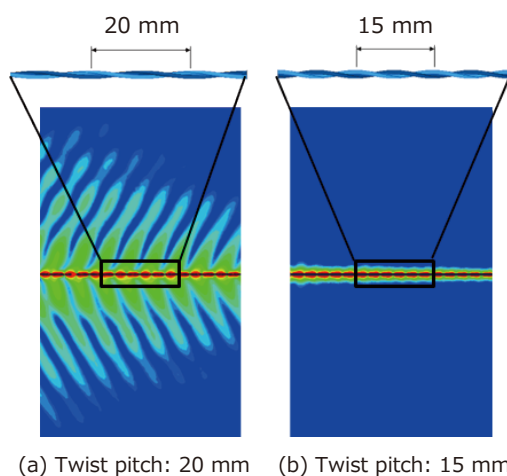(a) Twist pitch: 20 mm   (b) Twist pitch: 15 mm

Fig. 12. Difference in the electric field distribution due to the difference in the twist pitch at 6 GHz

5. Conclusion

We confirmed through experiments and simulation that structure-induced unintentional radiation of electromagnetic waves occurs in the UTP cable. We demonstrated that the mechanism of the radiation can be explained based on the same concept as that of leaky cables and that equations can be established for the radiation band and radiation angle. Notably, the equations include the effective relative permittivity and twist pitch as parameters, making it possible to control the radiation band and radiation angle.

The UTP cable evaluated in this paper is characterized by a structure and dimensions that are generally used for wiring between in-vehicle communications devices. However, the overlap of the radiation band with the sub-6 bands of 5G is likely to lead to an EMC problem. This EMC problem can be avoided by shifting the radiation band of the UTP cable to frequencies higher than those of the sub-6 bands. We presented that reducing the twist pitch would be one measure.

In-vehicle 5G devices are expected to come into widespread use toward the realization of automated driving. It will become necessary to select and use UTP cables that do not cause EMC problems in the sub-6 bands. We hope that the study in this paper will serve as guidelines for selecting UTP cables.

• HFSS and 2D Extractor are registered trademarks or trademarks of ANSYS Inc. or its subsidiaries in the United States or other countries.

Technical Terms

∗1 EMC: Abbreviation for "electromagnetic compatibility." It refers to the performance of an electronic device whose electromagnetic noise does not affect surrounding devices and which can operate without being affected by electromagnetic noise from other devices.

∗2 Multi-gigabit: A transmission mode and standard whose transmission speed and rate (number of bits transmitted per second) is several gigabits (10^9) or more.

∗3 Differential signals: Signals that are transmitted by a differential transmission protocol, which is designed to transmit signals by the voltage between two signal wires, by applying mutually anti-phase currents to the two signal wires.

∗4 Vector network analyzer: A device for measuring the frequency characteristics of the passing and reflected power in a high-frequency network.

∗5 Electrical length: Length based on the wavelength of propagated electromagnetic waves. The electrical length in a vacuum is equal to the physical length (which is measured by a ruler). The wavelength in a general medium is shorter than that in a vacuum, and the electrical length in a medium is longer than the physical length.

∗6 Effective relative permittivity: Relative permittivity of a medium on the assumption that the space around the signal wires is filled with a uniform medium with the electrical characteristics of the actual signal wires kept

intact. In general, it is a value between the relative permittivity of the coating resin and the relative permittivity of a vacuum ($\varepsilon_{r0} = 1$).

References

(1) M. Shafi, A. F. Molisch, P. J. Smith, T. Haustein, P. Zhu, P. De Silva, F. Tufvesson, A. Benjebbour, and G. Wunder, "5G: A tutorial overview of standards, trials, challenges, deployment, and practice," IEEE J. Sel. Areas Commun., vol. 35, no. 6, pp. 1201–1221 (Jun. 2017)

(2) C. R. Storck and F. Duarte-Figueiredo, "A survey of 5G technology evolution, standards, and infrastructure associated with vehicle-to-everything communications by internet of vehicles," IEEE Access, vol. 8, pp. 117 593–117 614 (2020)

(3) D. Okano, S. Yamashita, "Book of noise countermeasures to understand on site," Ohmsha, pp. 128-129 (2010) (Genba de wakaru noise taisaku no hon in Japanese)

(4) N. Tago, H. Ichimiya, Y. Amano, H. Satani, M. Ishikawa, and Y. Miyamoto, "Development of the Radiating Pair Cable (RPC)," SEI TECHNICAL REVIEW No.123, pp. 106-112 (Sept. 1983)

(5) S. Igarashi, D. Miyawaki, S. Yamagishi, I. Kuwayama, K. Iokibe, and Y. Toyota, "Unintentional radiated emissions from unshielded twisted pair cable attributed to twist structure," The 2021 IEICE general conference, B-4-3 (March 2021)

(6) S. Igarashi, D. Miyawaki, S. Yamagishi, I. Kuwayama, K. Iokibe, and Y. Toyota, "Unintentional radiated emissions from unshielded twisted pair cable attributed to twist structure," IEICE Communications Express, Vol. 11, No. 11, pp. 691-696 (2022)

Contributors   The lead author is indicated by an asterisk (∗).

S. IGARASHI∗
• Autonetworks Technologies, Ltd.

D. MIYAWAKI
• Group Manager, Autonetworks Technologies, Ltd.

S. YAMAGISHI
• Department Manager, Autonetworks Technologies, Ltd.

I. KUWAYAMA
• Senior Manager, Autonetworks Technologies, Ltd.

K. IOKIBE
• Associate Professor, Okayama University

Y. TOYOTA
• Professor, Okayama University

Clarification of the Mechanism of Unintentional Radiated Emissions from Unshielded Twisted Pair Cable